

# Synthesis and sintering behaviour in $\text{CeO}_2\text{-ZrO}_2$ ceramics

JENQ-GONG DUH, HSING-TAO DAI, WEI-YUUNG HSU

*Department of Materials Science and Engineering, National Tsing Hua University, Hsinchu, Taiwan*

The co-precipitation method has been employed to prepare  $\text{CeO}_2\text{-ZrO}_2$  ceramics. The application of a wet chemical method is expected to yield highly sinterable material at lower sintering temperatures. The characteristics of the synthesized powders are evaluated with respect to the particle size distribution, calcination step, and the degree of agglomeration. The sintering behaviour of the prepared powder is studied at various temperatures to obtain different phase distributions and grain sizes. The amount of the monoclinic phase in the as-sintered specimen is decreased with increasing  $\text{CeO}_2$  contents in  $\text{CeO}_2\text{-ZrO}_2$ . 13.7 mol%  $\text{CeO}_2$  is sufficient to achieve a tetragonal phase in the  $\text{CeO}_2\text{-ZrO}_2$  system. In addition,  $\text{Y}_2\text{O}_3$  and  $\text{MgO}$  dopants in  $\text{CeO}_2\text{-ZrO}_2$  reduce the grain size and result in a fully tetragonal phase for the 10 mol%  $\text{CeO}_2$  matrix.

## 1. Introduction

The  $\text{Y}_2\text{O}_3\text{-ZrO}_2$  type of ceramic is considered to be one of the toughest and strongest of the  $\text{ZrO}_2$  system [1-3]. The main deficiency of tough  $\text{Y}_2\text{O}_3\text{-ZrO}_2$  ceramics is an undesirable tetragonal-to-monoclinic transformation at low temperature in humid atmospheres or hot aqueous solutions [4-8]. Much attention has been paid to ceria-doped zirconia as a potential material for tough ceramics. It is believed that the thermal stability of zirconia could be improved by lowering the tetragonal-to-monoclinic transformation temperature. As the transformation temperature of ceria-doped zirconia is relatively low, it is a good candidate for improving the thermal stability. Several studies have proved that  $\text{CeO}_2$  is a better dopant than  $\text{Y}_2\text{O}_3$  in tetragonal zirconia polycrystal (TZP) from the viewpoint of toughness [9] and thermal stability [10].

The purpose of this study was first to fabricate  $\text{CeO}_2\text{-ZrO}_2$  powders by a chemical approach in order to obtain a highly sinterable body. The sintering behaviour of specimens with various ceria contents is investigated at different temperatures. The microstructure evolution of the as-sintered specimen is examined with the aid of the scanning electron microscope. In addition, the effect of  $\text{MgO}$  and  $\text{Y}_2\text{O}_3$  dopants in the  $\text{CeO}_2\text{-ZrO}_2$  will also be discussed.

## 2. Experimental procedure

$\text{CeO}_2\text{-ZrO}_2$  ceramics with ceria contents of 10, 11, 12 and 13.7 mol% were prepared by the co-precipitation process. The starting materials were  $\text{ZrOCl}_2 \cdot 8\text{H}_2\text{O}$  and  $\text{Ce}(\text{NO}_3)_3 \cdot 6\text{H}_2\text{O}$ . The hydroxide precursor was precipitated by adding  $\text{NH}_4\text{OH}$  solution to keep the process at  $\text{pH} = 9.1$  to 9.3. The flow chart for the preparation of the powders is represented in Fig. 1. The amorphous powder was calcined at  $500^\circ\text{C}$  for 1 h

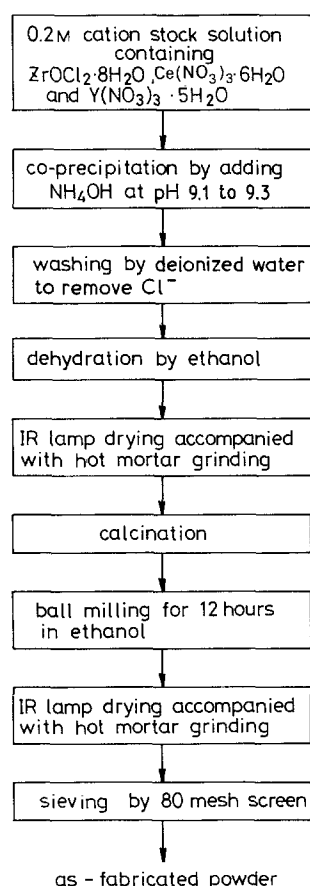


Figure 1 The preparation of  $\text{CeO}_2\text{-ZrO}_2$  powders.

and then wet-milled for 12 h in ethanol. The milled powder was granulated through 80-mesh screen and pressed into a pellet form with 10 mm diameter at a pressure of 87 MPa. The green compacts, about 40% theoretical density, were sintered in air at 1400 and  $1500^\circ\text{C}$  for various periods of time.

The bulk density of the sintered body was measured

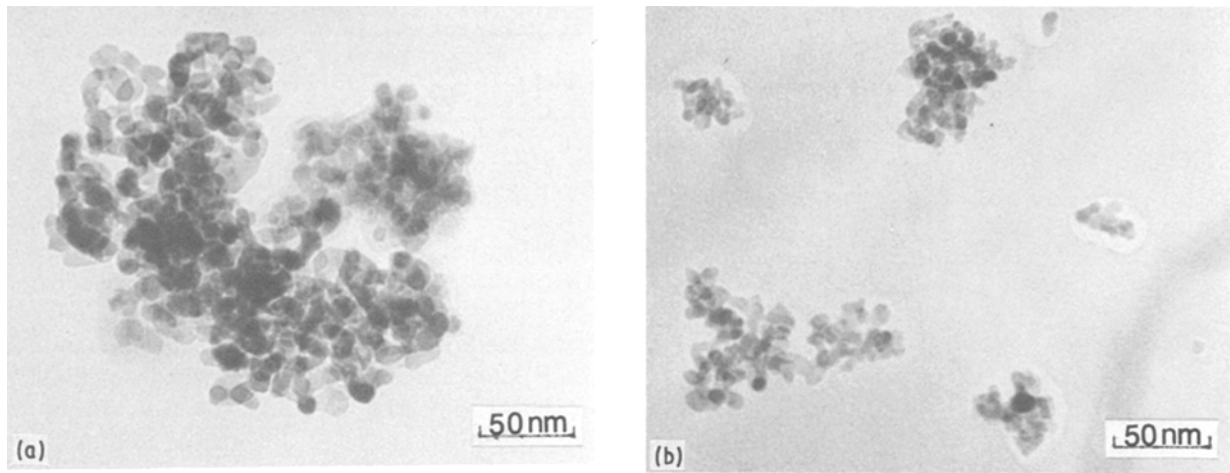


Figure 2 TEM micrographs of the as-fabricated powders with (a) 10 and (b) 12 mol % CeO<sub>2</sub>.

by the Archimedes technique in water. Phase identification was performed by X-ray diffraction and the fraction of monoclinic phase in the as-sintered body was evaluated by the equation [11]

$$\% \text{ monoclinic} = \frac{I(11\bar{1}_m) + I(111_m)}{I(11\bar{1}_m) + I(111_m) + I(111_t)} \quad (1)$$

where  $I(11\bar{1}_m)$ ,  $I(111_m)$  and  $I(111_t)$  represent the intensity in the monoclinic peaks  $(11\bar{1})$ ,  $(111)$  and tetragonal peak  $(111)$ , respectively. In addition, the microstructure evolution under various sintering conditions was examined with the scanning electron microscope (Hitachi S-570) and electron microprobe (Jeol JCSA-733).

### 3. Results and discussion

#### 3.1. Powder characteristics

The as-fabricated powder was calcined at 500°C for 1 h. The agglomerate structures of calcined powders were examined with SEM. Fig. 2 shows transmission electron (TEM) micrographs for the as-calcined powder. The particle size is in the order of 10 nm. Fig. 3 represents the SEM images for calcined powders with 10.2, 12 and 13.7 mol % CeO<sub>2</sub>. There exists some degree of agglomeration after calcination. The powders were further characterized with a centrifugal particle-size analyser (Shimadzu SA-CP2). The particle size distribution of the CeO<sub>2</sub>-ZrO<sub>2</sub> powders after ball-

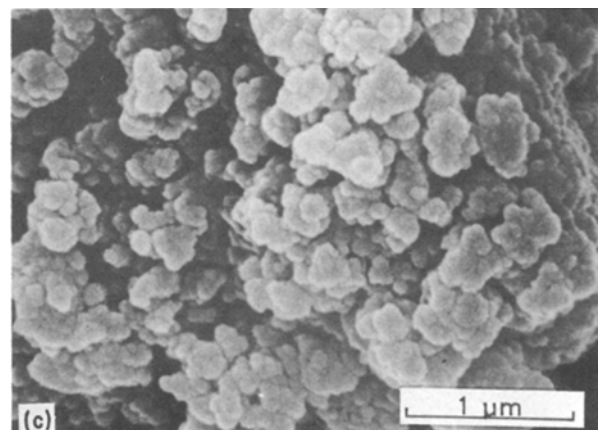
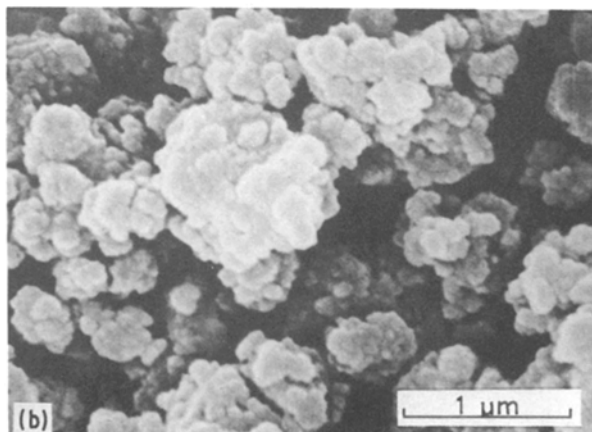
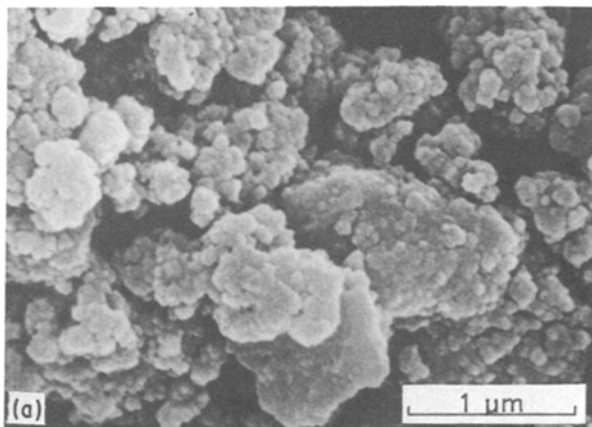


Figure 3 SEM images of powders calcined at 500°C for 1 h: (a) 10, (b) 12 and (c) 13.7 mol % CeO<sub>2</sub>.

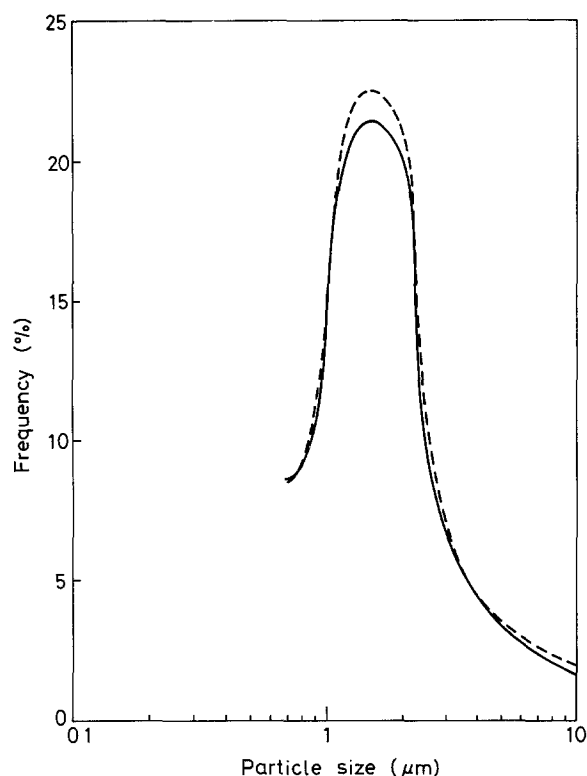


Figure 4 Particle size distribution of  $\text{CeO}_2\text{-ZrO}_2$  powders with (---) 2 mol %  $\text{YO}_{1.5}$  + 10 mol %  $\text{CeO}_2$  and (—) 10 mol %  $\text{CeO}_2$ .

milling is indicated in Fig. 4; the most probable particle size is found to be around 1  $\mu\text{m}$ .

### 3.2. Sintering studies

Sintering experiments were carried out at 1400 and 1500°C for various periods of time. A preliminary study of the sintering of  $\text{CeO}_2\text{-ZrO}_2$  has been reported by the authors [12]. Table I summarizes the specimen composition, sintering condition, sintered density and structure for the  $\text{CeO}_2\text{-ZrO}_2$  ceramics. The theoretical density was calculated from the measured lattice constants, which were derived from the X-ray diffraction pattern. Table II lists the calculated theoretical density obtained for compositions with 12 and 13.7 mol %  $\text{CeO}_2$ . Theoretical density calculations were not made for compositions with 10 and 11 mol %  $\text{CeO}_2$  as some

TABLE I Sintering data for  $\text{CeO}_2\text{-ZrO}_2$

Composition (mol % $\text{CeO}_2$ )	Sintering conditions	Density	% T.D.*	Structure†
10	1300°C, 3 h	5.3582	—	m
	1300°C, 5 h	5.3678	—	m
	1400°C, 1 h	5.4251	—	m
	1400°C, 3 h	5.4313	—	m
	1500°C, 3 h	—‡	—	m
11	1400°C, 3 h	5.99	—	t + m
	1500°C, 3 h	5.83	—	m + t
12	1400°C, 3 h	6.1509	98	t + m
	1400°C, 4.5 h	6.1644	98.4	t + m
	1400°C, 6.5 h	6.2582	99.9	t + m
	1500°C, 3 h	6.1962	99.0	t + m
13.7	1400°C, 3 h	6.1617	97.6	t

\*Theoretical density.

†m = monoclinic, t = tetragonal phase.

‡Pellet broken after sintering.

TABLE II Calculated theoretical density in  $\text{CeO}_2\text{-ZrO}_2$

Composition (mol % $\text{CeO}_2$ )	Lattice parameter (nm)		T.D. ( $\text{g cm}^{-3}$ )
	a	c	
12	0.51216	0.52238	6.259
13.7	0.51212	0.52145	6.3133

of the sintered pellets exhibited cracking after sintering. The purpose of preparing the ceramic powder by a chemical approach is to obtain a highly sinterable body. As expected, the as-fabricated powders in this study could achieve a high density in the as-sintered specimens. For the 12 mol %  $\text{CeO}_2$  specimen, the sintered density is 98% of theoretical density for 3 h sintering at 1400°C. Nearly complete theoretical density is expected after 6.5 h at 1400°C.

The density of powder with 10 mol %  $\text{CeO}_2$  is much lower than those of other compositions, as indicated in Table I. This is attributed to the existence of monoclinic phase. The relatively large specific volume of the monoclinic phase would introduce cracking in the as-sintered specimen, as shown in Fig. 5. Fig. 6 represents the fracture surface of powder with 10 mol %  $\text{CeO}_2$ . It is apparent that pores are trapped both between and within grains because of the rapid grain growth during sintering, which in turn results in the relatively low sintered density.

The X-ray diffraction patterns for specimens sintered at 1400°C for 3 h are shown in Fig. 7. It is found that 13.7 mol %  $\text{CeO}_2$  is sufficient to obtain a fully tetragonal phase. The fraction of monoclinic phase in as-sintered ceramics as a function of the  $\text{CeO}_2$  content is represented in Fig. 8. The monoclinic fraction decreases with increasing  $\text{CeO}_2$  content. This implies that the presence of  $\text{CeO}_2$  tends to stabilize the tetragonal phase, which is consistent with the  $\text{CeO}_2\text{-ZrO}_2$  phase diagram [13]. It is believed that  $\text{CeO}_2$  might stabilize the tetragonal phase by reducing the free energy of the tetragonal phase or increasing the constraints on phase transformation.

The microstructure of  $\text{CeO}_2\text{-ZrO}_2$  is revealed by the SEM and is represented in Fig. 9. There exists some degree of abnormal grain growth in the specimens, especially for the 10 mol %  $\text{CeO}_2$  composition. The

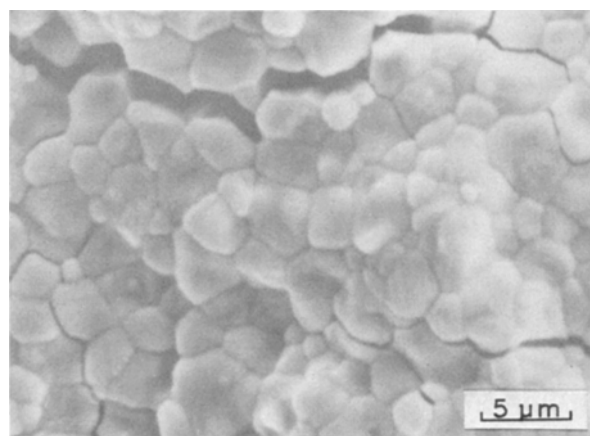


Figure 5 SEM image of the as-sintered surface for 10 mol %  $\text{CeO}_2$  specimen sintered at 1500°C for 3 h. Cracking is formed due to the monoclinic phase.

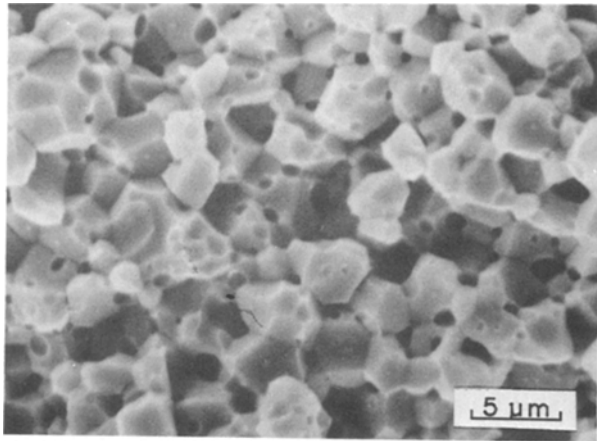


Figure 6 SEM image for the fracture surface of 10 mol% CeO<sub>2</sub> specimen sintered at 1500°C for 3 h. A pore trapped within the grain is visible.

average grain sizes after sintering at 1400°C for 3 h are 2 and 1 μm for 10 and 13.7 mol% CeO<sub>2</sub>, respectively, as shown in Figs 9a and b. The grain sizes in Figs 9c and d are estimated to be 2 and 4 μm for 12 and 11 mol% CeO<sub>2</sub>, respectively, after sintering at 1500°C for 3 h. It appears that the grain size of the sintered specimen decreases somewhat with increasing CeO<sub>2</sub> content in the ceramic. This observation is, however, different from the work by Tsukuma [14], who prepared TZP with 12 to 16 mol% CeO<sub>2</sub> by the hydrolysis technique with an aqueous solution of ZrOCl<sub>2</sub> and CeCl<sub>3</sub>. It was reported that the shape and size of grain were invariant with changes of CeO<sub>2</sub> content. The

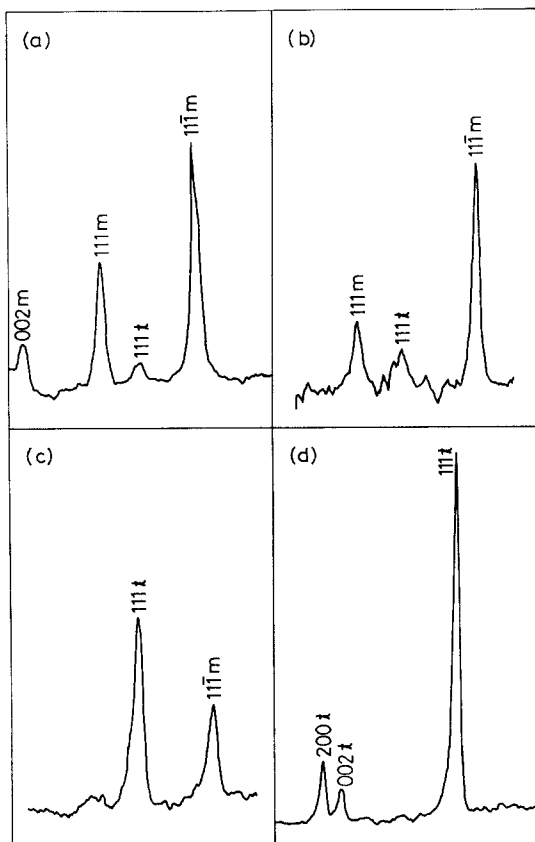


Figure 7 X-ray diffraction patterns for CeO<sub>2</sub>-ZrO<sub>2</sub> ceramics sintered at 1400°C for 3 h: (a) 10, (b) 11, (c) 12 and (d) 13.7 mol% CeO<sub>2</sub>.

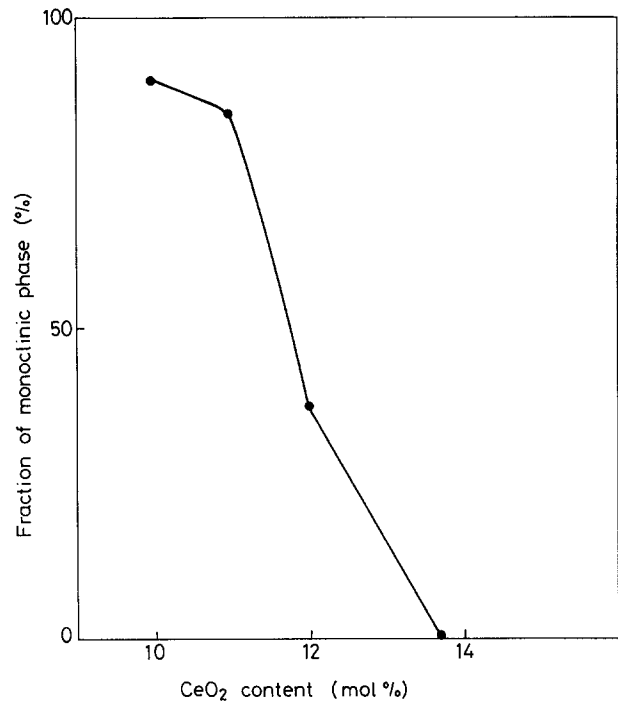


Figure 8 The fraction of monoclinic phase as a function of CeO<sub>2</sub> content.

discrepancy between this work and Tsukuma's work may be attributed to the different fabrication process and the composition range of CeO<sub>2</sub>.

### 3.3. The effect of Y<sub>2</sub>O<sub>3</sub> and MgO dopants

Fig. 10 shows the SEM image for a specimen with 1 mol% Y<sub>2</sub>O<sub>3</sub> and 10 mol% CeO<sub>2</sub>, sintered at 1400°C for 3 h. The grain size is smaller as compared to the 10 mol% CeO<sub>2</sub> specimen. In addition, the introduction of Y<sub>2</sub>O<sub>3</sub> dopants results in a fully tetragonal phase, as shown in the X-ray diffraction pattern of Fig. 11. A similar observation is made for MgO additives. Fig. 12 shows the microstructures for specimens with 2 mol% MgO and 10 mol% CeO<sub>2</sub>. The grain size for an MgO-doped specimen sintered at 1400°C for 5 h is less than 1 μm, as indicated in Fig. 12a. For a higher sintering temperature, at 1500°C for 3 h, (Fig. 12b) the grain size still remains in the range of 1 μm, which is even smaller than that for the 10 mol% CeO<sub>2</sub> specimen sintered at the lower temperature of 1400°C, as shown in Fig. 9a.

As indicated in Table I, the 12 mol% CeO<sub>2</sub> specimen exhibits a mixed phase of tetragonal and monoclinic structure. However, the addition of 2 mol% MgO and 1 mol% Y<sub>2</sub>O<sub>3</sub> to the 10 mol% CeO<sub>2</sub> specimen results in a fully tetragonal phase and smaller grain size. This suggests that MgO and Y<sub>2</sub>O<sub>3</sub> are stronger stabilizers for the tetragonal phase as compared to CeO<sub>2</sub>.

## 4. Conclusions

1. When the co-precipitation process is employed to derive CeO<sub>2</sub>-ZrO<sub>2</sub> ceramics with various CeO<sub>2</sub> contents, 13.7 mol% CeO<sub>2</sub> is sufficient to achieve a fully tetragonal phase.

2. The amount of monoclinic phase in the as-sintered CeO<sub>2</sub>-ZrO<sub>2</sub> specimen decreases with increasing content of CeO<sub>2</sub>.

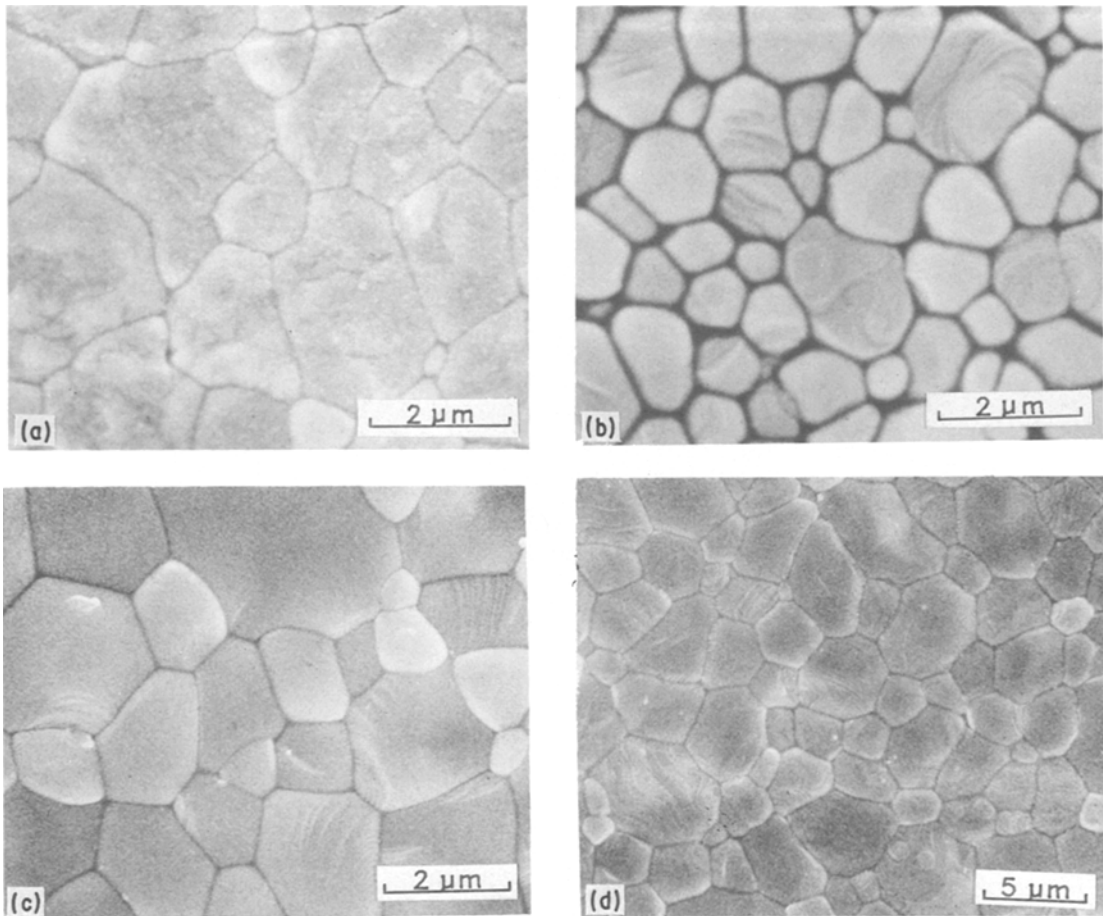


Figure 9 SEM images for as-sintered  $\text{CeO}_2\text{-ZrO}_2$  made under various conditions: (a) 10 mol %  $\text{CeO}_2$ , 1400° C for 3 h; (b) 13.7 mol %  $\text{CeO}_2$ , 1400° C for 3 h; (c) 12 mol %  $\text{CeO}_2$ , 1500° C for 3 h; (d) 11 mol %  $\text{CeO}_2$ , 1500° C for 3 h.

3. The powder made by a chemical approach results in a highly sinterable body. The 12 mol %  $\text{CeO}_2$  ceramic can reach nearly complete densification when sintered at 1400° C for 6.5 h.

4. 1 mol %  $\text{Y}_2\text{O}_3$  and 2 mol %  $\text{MgO}$  dopants in the  $\text{CeO}_2\text{-ZrO}_2$  system reduce the grain size of the as-sintered body and result in a fully tetragonal phase in the 10 mol %  $\text{CeO}_2$  matrix.

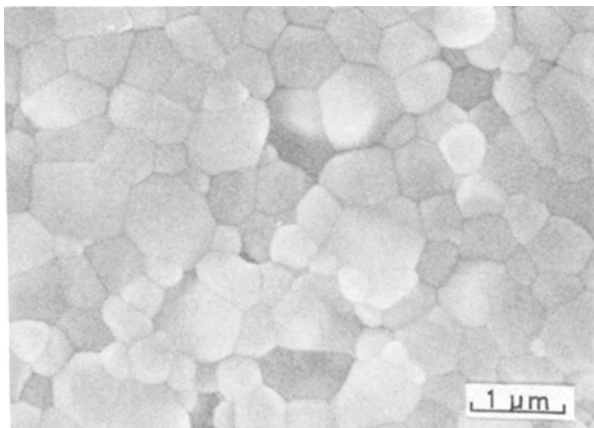


Figure 10 SEM micrograph for specimen with 1 mol %  $\text{Y}_2\text{O}_3$  and 10 mol %  $\text{CeO}_2$  sintered at 1400° C for 3 h.

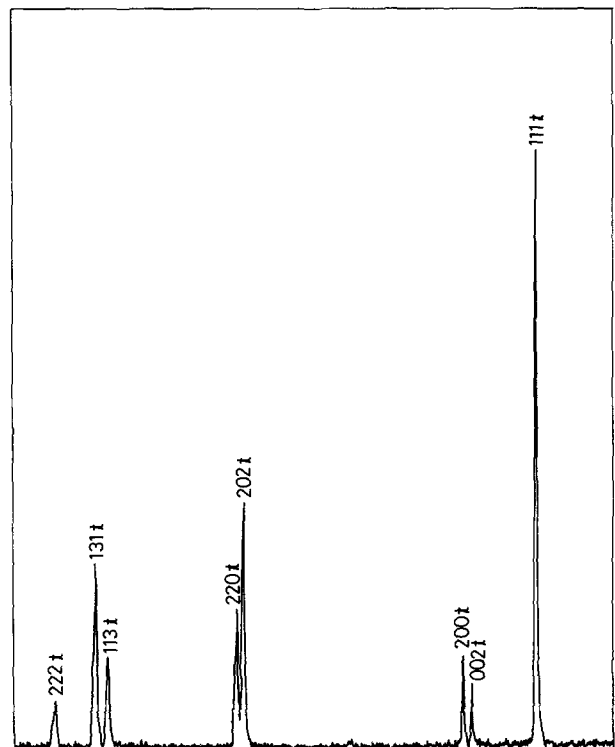


Figure 11 X-ray diffraction pattern for specimen with 1 mol %  $\text{Y}_2\text{O}_3$  and 10 mol %  $\text{CeO}_2$ , sintered at 1400° C for 3 h.

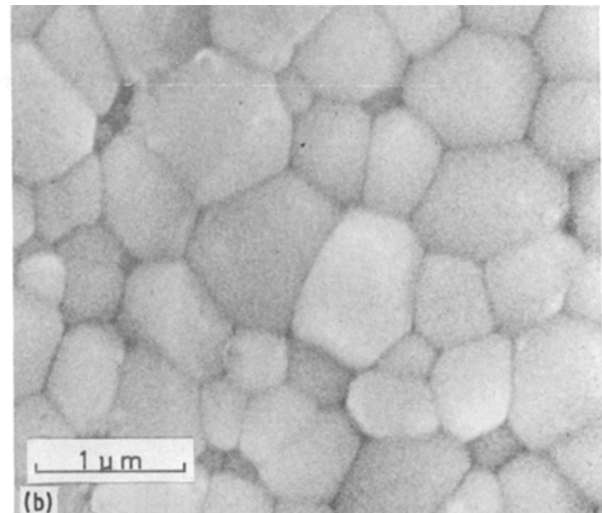
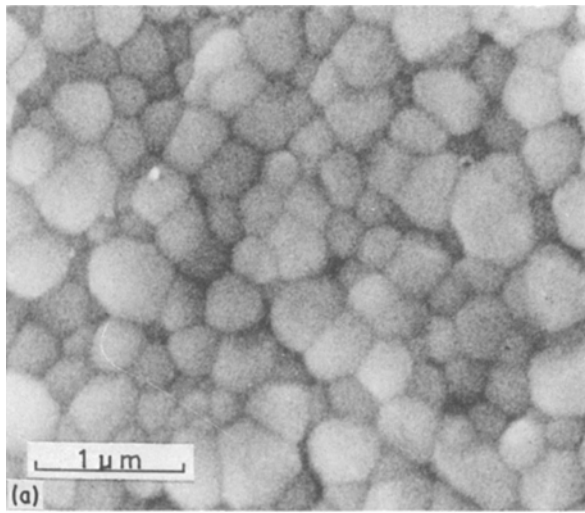


Figure 12 SEM micrographs for specimens with 2 mol % MgO and 10 mol % CeO<sub>2</sub> (a) sintered at 1400°C for 5 h, (b) sintered at 1500°C for 3 h.

### Acknowledgements

The authors wish to thank the National Science Council, Taiwan, for financial support under Contract No. NSC76-0405-E007-12. They are also indebted to Professor Bi-Shiou Chiou for helpful discussions throughout the course of this work.

### References

1. N. CLAUSSEN, in "Science and Technology of Zirconia II", edited by N. Claussen, M. Rühle and A. H. Heuer (American Ceramic Society, Columbus, Ohio, 1984) p. 325.
2. R. C. GARVIE, R. H. HANNINK and R. T. PASCOE, *Nature* **258** (1975) 703.
3. A. G. EVANS, D. B. MARSHALL and N. H. BURLINGAME, in "Science and Technology of Zirconia", edited by A. H. Heuer and L. W. Hobbs (American Ceramic Society, Columbus, Ohio, 1981) p. 202.
4. M. MATSUI, T. SOMA, T. OTAGIRI and I. ODA, *Amer. Ceram. Soc. Bull.* **60** (3) (1981) 382.
5. K. KOBAYASHI, K. KUWAJIMA and T. MASAKI, *Solid State Ion* **3-4** (1981) 489.
6. T. SATO and M. SHIMADA, *J. Amer. Ceram. Soc.* **67** (10) (1984) C212.
7. *Idem, ibid.* **68** (6) (1985) 356.
8. T. SATO, S. OHTAKI and M. SHIMADA, *J. Mater. Sci.* **20** (1985) 1466.
9. J. G. DUH, W. Y. HSU and B. S. CHIOU, in "High Tech Ceramics", Materials Science Monographs 38B, edited by P. Vincenzini (Elsevier, Amsterdam, 1987) p. 1281.
10. T. SATO, S. OHTAKI, T. ENDO and M. SHIMADA, *J. Mater. Sci. Lett.* **5** (1986) 1140.
11. H. TORAYA, M. YOSHIMURA and S. SOMIYA, *J. Amer. Ceram. Soc.* **67** (6) (1984) C-119.
12. B. S. CHIOU, W. Y. HSU and J. G. DUH, in Proceedings of 3rd International Conference on the Science and Technology of Zirconia, Tokyo, (Ceramic Society of Japan, Tokyo, 1986) p. 180.
13. E. TANI, M. YOSHIMURA and S. SOMIYA, *J. Amer. Ceram. Soc.* **66** (7) (1983) 506.
14. K. TSUKUMA, *Amer. Ceram. Soc. Bull.* **65** (10) (1986) 1386.

Received 12 August  
and accepted 1 December 1987